Mechanism of Tension Generation in Muscle: An Analysis of the Forward and Reverse Rate Constants

Julien S. Davis and Neal D. Epstein
Molecular Physiology Section, Laboratory of Molecular Cardiology, National Heart Lung and Blood Institute, National Institutes of Health, Bethesda, Maryland

ABSTRACT Tension generation in muscle occurs during the attached phase of the ATP-powered cyclic interaction of myosin heads with thin filaments. The transient nature of tension-generating intermediates and the complexity of the mechanochemical cross-bridge cycle have impeded a quantitative description of tension generation. Recent experiments performed under special conditions yielded a sigmoidal dependence of fiber tension on temperature—a unique case that simplifies the system to a two-state transition. We have applied this two-state analysis to kinetic data obtained from biexponential laser temperature-jump tension transients. Here we present the forward and reverse rate constants for de novo tension generation derived from analysis of the kinetics of the fast laser temperature-jump phase τ_2 (equivalent of the length-jump phase 2_{slow}). The slow phase τ_3 is temperature-independent indicating coupling to rather than a direct role in, de novo tension generation. Increasing temperature accelerates the forward, and slows the reverse, rate constant for the creation of the tension-generating state. Arrhenius behavior of the forward and anti-Arrhenius behavior of the reverse rate constant is a kinetic signature of multistate multipathway protein-folding reactions. We conclude that locally unfolded tertiary and/or secondary structure of the actomyosin cross-bridge mediates the power stroke.

INTRODUCTION

A hallmark of tension generation in striated muscle is that tension rises as temperature increases. Therefore, an endothermic (heat-absorbing), entropy driven (order-disorder) reaction generates tension in muscle. Assuming a tractable mechanism, co-analysis of the temperature dependencies of fiber isometric tension and the kinetics of tension generation should rigorously characterize the process. First indications that tension generation could be simplified and treated as single-step isomerization came from the observation of an apparent two-state dependence of fiber isometric tension on temperature (1). The term ''apparent'' is used to indicate that simple two-state behavior is manifested by a more complex ATP-driven mechanochemical cycle functioning within the crystal-like structure of the sarcomere. The thesis of this article is that by using the simplest of kinetic models, temperature dependencies of the forward and reverse rate constants of tension generation can be determined to give insights into the physical mechanism of tension generation in muscle.

The swinging lever-arm mechanism is considered to generate tension in muscle (2). In this model, the proximal catalytic domain of the myosin head is firmly attached to actin while the distal lever-arm domain swings some 60° in a power-stroke to generate tension and movement. Thus, localized structural changes in the actin-attached proximal region of the head are communicated to, and amplified by, the distal tail or lever-arm. At the level of the sarcomere, the ATP-driven contractile cycle is mediated by myosin heads, which extend from the thick filament backbone and asynchronously attach, generate tension, and detach from adjacent actin thin filaments. The cycle is initiated by the tight binding of ATP (T) to the actomyosin rigor complex. This interaction dissociates myosin from actin and reverses the power stroke. Hydrolysis of ATP to a myosin, ADP (D), and P_i (P) ternary complex (MDP) follows. Both MTP and MDP states have similar affinities for actin. However, the actin-catalyzed release of phosphate with its associated large free energy change drives the reaction forward to favor the formation of AMD attached states (3). Tension generation is linked to this free energy change associated with P_i release, but opinion is divided as to whether the transition occurs before (4–6), during (7,8), or after (9–13) P_i release. Discharge of cross-bridge tension by movement and rotation of the myosin tail facilitates the strain-sensitive dissociation of ADP to complete the cycle.

Kinetic experiments on contracting muscle fibers provide a powerful technique to probe both the mechanism of de novo tension generation (creation of a tension generating state from a pretension generating state) and its location within the cross-bridge cycle. Of the different kinetic techniques employed, small perturbations applied to maximally Ca^{2+} activated single muscle fibers contracting isometrically are the method of choice to quantify and characterize mechanical tension transients (14,15). One important reason is that the interconversion of intermediate states before and after rate-limiting steps are probed simultaneously as exponential processes. In contrast, a large-perturbation initiates a process in which reaction steps are probed sequentially to provide information up to, but not beyond, the rate-limiting step. Small perturbations also enable nonlinear (second and higher order in concentration) differential rate equations to be linearized (pseudo-first order in concentration). Small-perturbation

Submitted November 20, 2006, and accepted for publication January 4, 2007.

Address reprint requests to Julien S. Davis, Tel.: 301-435-5285; E-mail: davisjs@nhlbi.nih.gov.

0006-3495/07/04/2865/10 $2.00

doi: 10.1529/biophysj.106.101477

methods commonly used in muscle research include laser temperature-jump (T-jump), length-jump (L-jump), pressure-jump (P-jump), and the various concentration jumps (released from precursor ''caged'' compounds by photolysis) that include phosphate-jump (P_i-jump) and adenosine diphosphate jump (ADP-jump) experiments (e.g., Table 2 in (12)). Of all available methods, classical L-jump experiments generate the most complex kinetic response consisting of four exponential phases (phases 2_{fast}, 2_{slow}, 3, and 4) and one amplitude (phase 1). L-jump tension transients are commonly used as the reference system because all intermediate states that generate tension or bear tension, either transiently or continuously, are perturbed. In contrast to homogeneous reactions in solution, exponential kinetic phases in muscle fibers can arise from two distinct sources:

1. Perturbation of the contractile cycle (tension generation, and the cyclic hydrolysis of ATP by the actomyosin ATPase).
2. Perturbation of the viscoelastic properties of the muscle proteins, processes defined as largely independent of the structural changes associated with the cross-bridge cycle.

Accordingly, in L-jump experiments, phases 2_{slow}, 3, and 4 are a product of the contractile cycle, while phases 1 and 2_{fast} arise from the elastic/viscoelastic properties of the proteins (see (15)). The laser T-jump used in the experiments described here results in a much simpler kinetic response. This is because relative movement of thick and thin filaments is virtually eliminated in laser T-jump experiments on contracting muscle fibers. Thus, T-jump phases τ_2 and τ_3 are the direct result of the step change in temperature, and are respectively equivalent to L-jump phases 2_{slow} and 4 (10,16). The fastest of the phases, the small-amplitude τ_1 is the product of a mini L-jump imposed by thermal expansion of the fiber, and is considered an indirect consequence of the T-jump. Of the T-jump phases, only τ_2 and its equivalent L-jump phase 2_{slow} are considered associated with de novo tension generation (10,16). Unique temperature dependencies of the kinetics enable individual exponential T-jump and L-jump phases (and phases from other small ''jump'' experiments) to be cross-correlated with a high degree of certainty (e.g., Table 2 in (12)).

To make tension generation tractable for analysis in this study, we use data obtained from rabbit psoas fast fibers in the presence of low concentrations of ADP and P_i. Under these conditions, tension plotted against temperature is sigmoidal in form thus approximating a two-state single-step reaction between pre-force-generating and force-generation states (1). The relationships between the T-jump phase τ_2 and fiber tension is analyzed quantitatively to give the forward and reverse rate constants of tension generation. Arrhenius plots of these rate data provide the activation enthalpy and entropy values for tension generation and its reversal. Activation parameters are useful because they provide insights into the nature of the structural changes that occur on tension generation. This is achieved by comparing the $\Delta H^{\ddagger}$ and $\Delta S^{\ddagger}$ values for the forward and reverse rates of tension generation with data in the protein self-assembly, conformational change, and folding literature. A preliminary account of these experiments has appeared in abstract form (17).

MATERIALS AND METHODS

The design of the laser T-jump, the preparation of detergent-skinned muscle fibers, the method of activation and of data analysis are described in detail elsewhere (10,15,16). Rabbits were sacrificed under NHLBI Animal Care and Use Protocol 2-MC-30(R). The ionic strength of the solutions was 0.2 M and were the same as those used by Davis and Harrington (10). Glycerol 2-phosphate is used as a temperature-insensitive buffer at pH 7.1.

Determination of the forward and reverse rate constants for tension generation

The temperature dependence of isometric tension and the kinetics of tension are treated as an approximate two-state transition:

$$A \underset{k_1}{\overset{k_{-1}}{\leftrightarrows}} B. \tag{1}$$

A is the pre-force-generating state, B is the force-generating state, and isometric tension is used as a measure of the concentration of B. We initially reasoned that tension per cross-bridge would change little over the temperature range used, since polymer elasticity is generally proportional to absolute temperature (1). Optical trap experiments support this by showing that tension per head of both myosin (18) and kinesin (19) appears temperature-independent, validating the approximation. Thus, the tension versus temperature data is fitted to the two-state model isomerization of Eq. 1. Here the apparent equilibrium constant K_T at a particular temperature T is determined by ΔH^o (enthalpy change), T_m (transition midpoint temperature), P_∞ (tension at infinite temperature), and A_0 (the total concentration of actin-attached pre-force- and force-generating states):

$$K_T = [B]/[A] = k_1/k_{-1} = \exp((-\Delta H^o/R)(1/T - 1/T_m)). \tag{2}$$

The parameters ΔH^o, T_m, and P_∞ were obtained from the tension versus temperature data using nonlinear least-squares analysis and the relationships

$$P_\infty = [A_0] = [A] + [B] \tag{3}$$

$$[B] = [A_0] - [A_0]/(1 + \exp((-\Delta H^o/R)(1/T - 1/T_m))). \tag{4}$$

The observed rate constant or reciprocal relaxation time $1/\tau_2$ for the Eq. 1 mechanism is

$$1/\tau_2 = k_1 + k_{-1}. \tag{5}$$

Forward and reverse rate constants at a particular temperature are determined as (e.g., (20))

$$k_{-1} = 1/\tau_2/(K_T + 1), \tag{6}$$

$$k_1 = 1/\tau_2 - k_{-1}. \tag{7}$$

Activation energies (E_A) for the forward and reverse rate constants are determined from Arrhenius plots of the k_1 and k_{-1} rate constants where A is the preexponential factor, R is the gas constant, and T is absolute temperature (21):

$$k = A \exp(-E_A/RT). \tag{8}$$

Reformulation of the Arrhenius equation using transition-state theory for a first-order isomerization results in the relationship

$$k = (k_B T/h)\exp(\Delta S^{\ddagger}/R)\exp(-\Delta H^{\ddagger}/RT), \qquad (9)$$

where k_B is the Boltzmann constant, h is the Planck constant, $\Delta S^{\ddagger}$ is the entropy of activation, and $\Delta H^{\ddagger}$ is the enthalpy of activation (21,22).

RESULTS

We investigate the roles of the laser T-jump phases in tension generation and obtain the forward and reverse rate constants for tension generation from the two-state analysis of τ_2. To do this, quantitative relationships are established between fiber isometric tension and the kinetics. Two-state van' t Hoff analysis is used to obtain the thermodynamic parameters that govern steady-state fiber tension. Phase τ_2 amplitude data are compared directly with the temperature dependence of isometric tension to show a common origin. The key to this analysis is the temperature-dependent equilibrium constant (K_T) for tension generation, which is used to calculate the forward and reverse rate constants for tension generation from the observed rate constant ($1/\tau_2$) data obtained from laser T-jump experiments on single muscle fibers at different temperatures. Arrhenius plots of the temperature dependencies of the forward and reverse rate constants for tension generation provide their respective activation parameters $\Delta G^{\ddagger}$, $\Delta H^{\ddagger}$, and $\Delta S^{\ddagger}$. Transition state theory is applied to show that thermodynamic parameters ΔG^{o}, ΔH^{o}, and ΔS^{o} for the two-state temperature dependence of fiber tension relate quantitatively to the activation parameters obtained from the kinetics.

Temperature dependence of isometric tension

We apply a method used earlier (1) to characterize the sigmoidal dependence of isometric tension on temperature (Fig. 1). These data are sourced from the same article of Ranatunga's (23) as are the T-jump kinetics we later analyze in conjunction with our own T-jump data. The van't Hoff equation and the two-state mechanism of Eq. 1 were used to obtain the thermodynamic parameters governing fiber tension listed in the figure legend. The data set used first (1) proved to have an anomalously high T_m of 14.5°C, while the T_m of 9.9 ± 0.6°C for the reaction midpoint obtained here is comparable to the ~8°C value determined under similar conditions in more recent work (24).

Laser T-jump tension transients

Kinetic data were obtained by applying a small 5°C step increase in temperature to a fiber contracting under isometric conditions. Temperature-sensitive steps in the cycle are simultaneously perturbed by a small amount. The resulting tension transient arises from the kinetically controlled adjustment of the steady state to new conditions at the higher temperature and has the typical form of the sum of a series of exponential processes (or relaxations) (23,25,26). Laser T-jump tension transients consist of three exponential phases (Fig. 2) of which only the slower two kinetic phases τ_2 (*orange*) and τ_3 (*green*) arise from the effect of temperature on the cross-bridge cycle (10,23). As mentioned in the Introduction, the fastest phase, the small-amplitude τ_1 (*black*), is the product of a mini L-jump (instantaneous drop in tension) imposed by thermal expansion of the fiber and is considered an indirect consequence of the T-jump (10). We therefore exclude this small-amplitude, movement-induced phase from our analysis to focus on the heat-induced increase in fiber tension caused by the biphasic tension transient governed by τ_2 and τ_3.

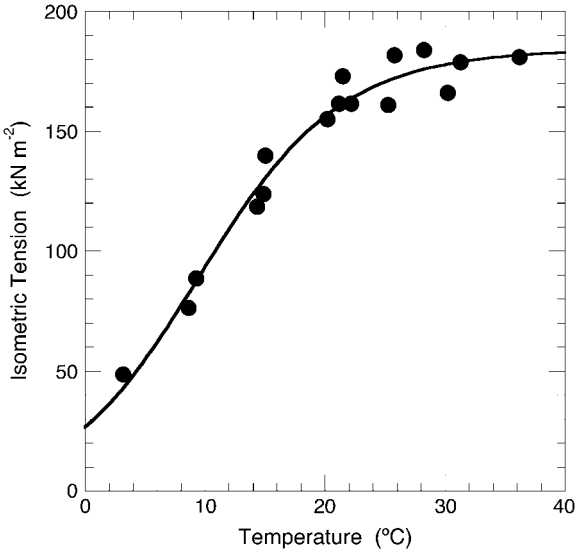

FIGURE 1 Temperature dependence of isometric tension analyzed as a two-state transition. The continuous line represents a nonlinear least-squares fit (1) to a single-step isomerization between pre-force-generating and force-generating states. Fitted parameters to the van' t Hoff equation were ΔH^{o} of 116.1 ± 13.6 kJ mol^{-1}, T_m of 9.9 ± 0.6°C and maximum tension 184 ± 5 kPa and $R = 0.984$. The entropy change (ΔS^{o}) was 410.6 ± 48.1 J K^{-1} mol^{-1}. Data were obtained from Fig. 4 *a* of Ranatunga (23).

Temperature dependencies of the rates and amplitudes of τ_2 and τ_3

Kinetic phases are defined by an observed rate constant and a reaction amplitude. Often rates alone are taken into consideration when deriving reaction mechanisms from experimental data. However, rigorous kinetic analysis gains from having both rate and amplitude data taken into account when formulating mechanisms.

Amplitude data is evaluated first, because it has a simple and direct relationship to temperature versus tension data (Fig. 1) in that the amplitudes of phases τ_2 (*orange*) and τ_3 (*green*) (Fig. 2) add to give the increase in isometric tension with temperature (1,10). It is evident from Fig. 3, that plots of amplitude versus temperature data for τ_2 (*orange*) and τ_3

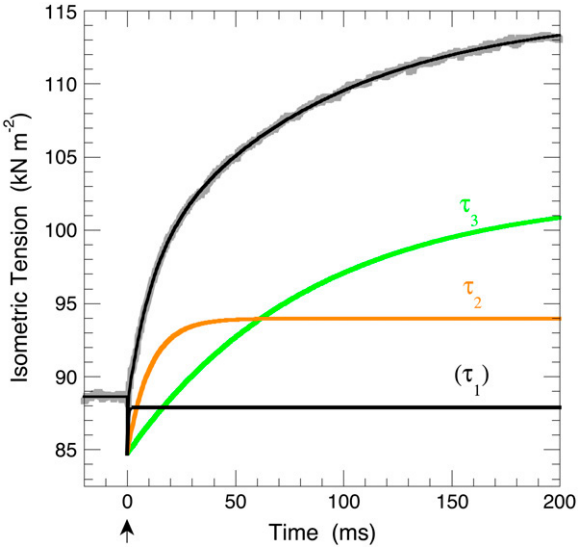

FIGURE 2 Laser T-jump tension transient. A single, skinned, maximally Ca^{2+} activated, rabbit psoas fiber contracting isometrically was heated by 5°C in <1 μs to a postjump temperature of 11°C at the arrow. Nonlinear least-squares fit to the sum of three exponentials was applied to the these data (10). Resolved fits to phases, τ_1, τ_2, and τ_3, are labeled and the overall fit (the sum of their amplitudes) is drawn as a solid line through shaded raw data. Adapted from Davis and Rodgers (11).

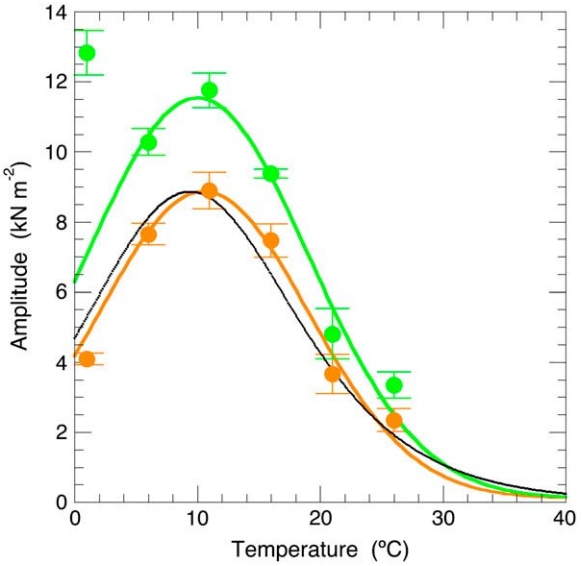

FIGURE 3 Temperature dependencies of the amplitude of τ_2. Bell-shaped, two-state dependence of amplitudes ($\Delta P_o/\Delta T$) of τ_2 (*orange*) and τ_3 (*green*) on prejump temperature. Comparison of T_m values obtained from Gaussian fits (1°C datum excluded) to the amplitudes of τ_2 (10.6 ± 0.8°C) and τ_3 (10.0 ± 1.1°C) with the first derivative ($\delta P_o/\delta T$, *black*) (9.9° ± 0.6°C) of the van' t Hoff fit to fiber tension (Fig. 1) indicates a common source of signal. Error bars are mean ± SE.

(*green*) have a common bell-shaped form. A remarkable feature of the amplitudes of the two kinetic phases is that the amplitude of τ_3 is a constant and temperature-independent 33.5 ± 2.2% greater than the corresponding τ_2 values at temperatures above 6°C (1). This causes a proportional vertical offset between these two otherwise identical bell-shaped curves (Fig. 3). Both, in turn, closely resemble the first derivative (instantaneous slope, Fig. 3, *black*) of the fit to the temperature dependence of isometric tension (Fig. 1). Thus, apart from differences in magnitude, each has the symmetrical bell-shaped form unique to the reversible single-step first-order reaction of Eq. 1. Comparable T_m values of ~10°C (the temperature at which K_T is unity) for τ_2, τ_3, and isometric tension (Fig. 3) indicate a specific single-step reaction as common origin. A mechanism for the departure of these amplitude data from the two-state scheme of Eq. 1 at temperatures below 6°C is discussed later. Based on these amplitude data alone, the simplest interpretation is that both kinetic phases could be directly involved in tension generation. Rate data is needed to further constrain the mechanism.

Temperature dependencies of observed rate constants for the two phases that comprise the T-jump tension transient are illustrated in Fig. 4. An Arrhenius plot of the apparent rate constant or reciprocal relaxation time of τ_2 (*orange*) illustrates the requisite temperature sensitivity for a source of fiber tension (10,11,23). Phase τ_3 fails the de novo tension-generation test because its rate is temperature-independent (*green*). This observation directly implies that the forward and reverse rate constants for the reaction are invariant with temperature; consequently, the equilibrium constant for that reaction is, by definition, temperature-independent. This behavior effectively excludes τ_3 from a direct role in a decidedly temperature-sensitive reaction like tension generation.

Forward and reverse rate constants of tension generation

The possibility of a two-state link between fiber tension and the rate of τ_2, the one remaining candidate tension-generating phase, is considered next. The simplest of mechanisms in which tension is generated by a fast isolated single-step isomerization (Eq. 1) in a slow steady-state cross-bridge cycle (Eq. 10) is used for analysis:

$$\rightarrow A \underset{k_1}{\overset{k_{-1}}{\leftrightarrows}} B \rightarrow . \qquad (10)$$

The relationship between $1/\tau_2$ the observed rate constant and the individual forward and reverse rate constants for such a tension-generating step is depicted in Eq. 5. Pairs of τ_2 (Fig. 4) and K_T (Fig. 1) values and Eqs. 6 and 7 were used to calculate the forward (k_1) and reverse rate constants (k_{-1}) for tension generation. The resultant Arrhenius plots of these rate data (Fig. 5) show k_1 to be accelerated by, and k_{-1} to be slowed (anti-Arrhenius behavior, characterized by an ''effective'' negative activation enthalpy), by increasing temperature. A characteristic of such kinetics is that the observed

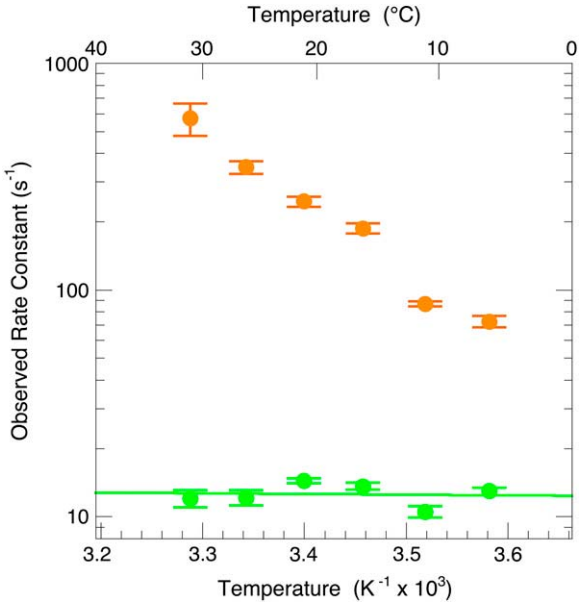

FIGURE 4 Temperature dependencies of the rates of τ_2 and τ_3. Arrhenius plot of the observed rate constants for phases τ_2 (*orange*) and τ_3 (*green*) versus postjump temperature. The temperature-independent rate constant of τ_3 (*green*) excludes this slow transition (12.6 ± 0.6 s^{-1}) from de novo tension generation (1,16). Error bars are mean ± SE. Adapted from Davis and Rodgers (11).

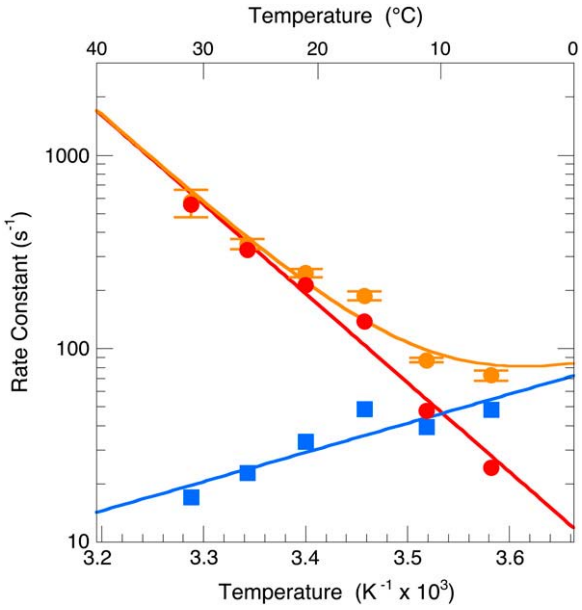

FIGURE 5 Arrhenius plots of the forward and reverse rate constants for tension generation. The rate of k_1 (*red*) increases with temperature while the rate of k_{-1} (*blue*) decreases (anti-Arrhenius behavior). The sum of the fits to the forward and reverse rate constants (*orange*) are drawn through $1/\tau_2$ values from Fig. 4. The forward and reverse rate constants for tension generation were calculated from the thermodynamic parameters governing the temperature dependence of fiber isometric tension (Fig. 1), and τ_2 values (Fig. 4). Rates for k_1 and k_{-1} were 168 and 30.3 s^{-1} (20°C) and 1728 and 14.1 s^{-1} (40°C), respectively. Activation parameters for k_1 were $\Delta H^{\ddagger} = 88.3$ kJ mol^{-1}, $\Delta S^{\ddagger} = 98.9$ J mol^{-1} K^{-1}, and $R = 0.993$; for k_{-1} $\Delta H^{\ddagger} = -28.9$ kJ mol^{-1}, $\Delta S^{\ddagger} = -315.2$ J mol^{-1} K^{-1}, and $R = 0.850$.

rate constant for τ_2 should first decline and then rise on cooling at an inflection point at the T_m of 9.9°C. This particular form of the curve is barely visible at the low temperature limit of the laser T-jump kinetic data in Fig. 5 (*orange*). Only the decline and plateau of the observed rate constant on cooling is evident in the raw data. However, the extrapolated fit to the 0°C (right-hand) intercept does show all the features. This is due in part to the relatively shallow slope of the reverse, as opposed to the forward rate constant. However, the expected full triphasic ''dog's leg,'' chevron, or V-shaped form is a distinctive feature of Arrhenius plots of the functionally equivalent L-jump phase 2_{slow} (10, 12)—primarily a consequence of the L-jump data extending down to a 5°C lower temperature. A similar analysis of these L-jump kinetic data is presented elsewhere (unpublished).

Transition-state theory provides the formal link between these rate constants and fiber tension. Activation enthalpy and entropy values (see Materials and Methods) for k_1 and k_{-1} are listed in Fig. 5. We also calculated $\Delta H^{\ddagger}$ and $\Delta S^{\ddagger}$ values using Ranatunga's independently obtained τ_2 rate data (Fig. 6 *a* in (23)). Values determined for k_1 were $\Delta H^{\ddagger} =$ 89.4 kJ mol^{-1} and $\Delta S^{\ddagger} = 99.8$ J mol^{-1} K^{-1}; and for k_{-1} $\Delta H^{\ddagger} = -26.8$ kJ mol^{-1} and $\Delta S^{\ddagger} = -310.9$ J mol^{-1} K^{-1}, all within a few percent of our own values (Fig. 5 and below). Granted the correct model, thermodynamic parameters can be calculated from the activation parameters for k_1 and k_{-1} with the equations $\Delta H^{o} = \Delta H^{\ddagger}_{k1} - \Delta H^{\ddagger}_{k-1}$ and $\Delta S^{o} = \Delta S^{\ddagger}_{k1} - \Delta S^{\ddagger}_{k-1}$. Thus, $\Delta H^{o} = 88.3 - (-28.9) = 117.2$ kJ mol^{-1} and $\Delta S^{o} = 98.9 - (-315.2) = 414.1$ J mol^{-1} K^{-1} values obtained from the kinetics are comparable to the directly determined thermodynamic parameters for ΔH^{o} of 116.1 ± 13.6 kJ mol^{-1} and ΔS^{o} of 410.6 ± 48.1 J K^{-1} mol^{-1} (Fig. 1). To conclude, it appears that both rates and amplitudes are consistent with apparent two-state tension generation by τ_2.

DISCUSSION

We have described experiments that relate the kinetics of tension generation to isometric force in muscle fibers. The rather remarkable observation that a single-step isomerization is sufficient to model the temperature-dependencies of fiber tension and the rate and amplitude of a particular kinetic phase has definite consequences for our understanding of the mechanism of muscle contraction.

Two-state tension generation in a steady-state pathway

Details of the kinetic and equilibrium behavior of the simple two-state isomerization are outlined under Materials and Methods. We have discovered conditions that allow tension generation by a normally complex and analytically intractable multistep contractile cycle to be reduced to an apparent single-step isomerization of the actomyosin cross-bridge.

The existence of such an experimental ''window'' requires that the tension-generating transition, in which the pre-force-generating state is converted to the force generating state, be largely insensitive to changes in other intermediate states of the cross-bridge cycle. Core requirements for this type of behavior by a single-step reaction in a steady-state cycle include: 1), the transition has to be fast compared with the overall rate of the cycle; and 2), changing temperature will alter the ratio of the pre-force-generating state to the force-generating state (tension changes with temperature), but the sum of the concentrations of the two states must remain constant. These two requirements are discussed next.

A muscle fiber contracting under isometric condition is in a steady state powered by the hydrolysis of ATP. To avoid significant bias to the observed rate constant of a two-state transition by flow, the rate of the transition has to be much faster than the flux through the functioning cycle. This requirement ensures that the reaction being characterized is close to equilibrium, and can be studied as such. A similar simplification was first used in the modeling tension generation by phase 2 in pioneering experiments some 35 years ago (27). In rabbit fast psoas fibers contracting under isometric conditions, flux or flow through the cross-bridge cycle is known to be slow (0.84 s^{-1} at 10°C (28), and 3.2 s^{-1} at 20°C (29)). These rate data assume all heads in a fiber generate tension. It is, however, probably wise to double these values, because it is likely that <50% of myosin heads are engaged in tension generation (30). We conclude that the flux through the cycle will only slightly affect the value of the ~50-fold faster forward rate constant (k_1) we record in our experiments.

The second requirement for two-state analysis of the amplitude of phase τ_2 and of fiber tension (but not rate data) is that the sum of the two participating intermediate states (pre-force-and force-generating) must remain constant regardless of temperature. This condition is met because the temperature dependence of the amplitude of τ_2 and τ_3 is bell-shaped above 5°C—the unique form of a single-step first-order reaction with a maximum where $K_T = 1$ and both reactants are equal in concentration. Were coupling to adjacent reactions to occur, the bell-shaped form would be distorted. We therefore conclude that all accessible myosin-binding sites on the thin filaments are fully occupied at and above 5°C. Rapid attachment of MDP cross-bridges to actin and a rate-limiting detachment of AMD cross-bridges probably serve to maintain saturation (see (31) and references therein). The decline in amplitude observed at 1°C (Fig. 4 and (1)) indicates that thin filaments are no longer saturated with myosin heads, and that the sum of the concentrations of the pre-force- and force-generating states has declined. A related discontinuity has been observed in the amplitude of phase 2_{slow}, the L-jump equivalent of τ_2, at low temperatures (10,12). Inspection of Eqs. 4 and 5 shows that two-state analysis of amplitudes, but not of rate data, fails under such conditions. The observed decline in saturation is probably the result of limiting concentrations of MDP heads ready to bind to actin. A plausible explanation is that both observations probably result from the temperature sensitivity of ATP hydrolysis by myosin where the equilibrium constant increases from 1.6 at 3°C to 7 at 20°C (32). Low temperatures favor the MT state, causing a reciprocal reduction in the concentration of the reactive MDP state. We conclude that actin is saturated with myosin heads at and above 5°C. Submaximal activation by Ca^{2+} at low temperatures might also contribute to the effect. Further support for this interpretation comes from the observation that instantaneous stiffness (a measure of the number of attached heads) is constant above 5°C but drops below this temperature (J. S. Davis, personal observation). Temperature dependencies like this, in which stiffness decreases at low temperatures and is constant at higher temperatures, have previously been described in rat fibers (33). A decrease in the number of strongly attached cross-bridges at low temperatures is consistent with this observation. In this instance, the exception has proved the rule, which is why two-state analysis of amplitude data is limited to 5°C and above.

Tension generation and the cross-bridge cycle

We now consider two-state tension generation in the wider context of an ATP-driven cross-bridge cycle. A central requirement for two-state analysis is that the tension-generating isomerization must be independent of, and thus unaffected by, kinetic or equilibrium coupling/linkage to all upstream and downstream steps in the cycle. It must, apart from the slow steady-state flux through the reaction, function as a reaction in isolation (Eq. 10). As discussed, all that is required to maintain two-state tension generation in general is: 1), a slow unidirectional flux in and out of a faster tension-generating isomerization; and 2), the sum of the pre-force- and force-generating states must remain constant. Tension generation by muscle fibers is governed at two different levels of organization: One is the ATP-driven biochemical pathway that largely determines the sequence and rates of interconversion of various intermediate states of by actin and myosin during the cross-bridge cycle. The other concerns mechanical coupling/cooperativity between ensembles of cross-bridges imposed by the paracrystalline array of overlapping thick and thin filaments in the sarcomere (27,34–36). We show that under the stringent mechanochemical constraints of our experiments these potentially complicating issues, from known properties of the mechanochemical cross-bridge cycle, have little affect on the manifestation of single-step tension generation and on the rate constants we determine for tension generation. The location of the tension-generating step within the cross-bridge cycle is considered first, since it is key to analysis.

Under conditions of steady-state ATP hydrolysis, the mechanochemical cycle can be subdivided into groups of steps close to equilibrium separated by irreversible or rate-limiting

steps. Each exponential phase arises from a primary transition/step in the cycle. The rules are straightforward for ordering the sequence in which kinetic phases occur: Two kinetic steps are linked and in the same group of reactions if they are kinetically coupled (occur on the same timescale) or equilibrium-coupled (fast steps equilibrate before slow steps) to one another. They are in different groups if they appear linked in only one direction by flux through an irreversible step. We show that tension generation functions alone in its own group under our experimental conditions. Low concentrations of P_i are used here to minimize the mass-action-driven accumulation of intermediates before its release. A manifestation of the effect of P_i is seen when simple two-state analysis of the effect of temperature on isometric tension fails when P_i is added to a contracting fiber (24). As mentioned, P_i depresses fiber stiffness and isometric tension signaling a desaturation of the thin filaments by myosin. Rigor bridge accumulation is minimized by maintaining low concentrations of ADP. Mechanical coupling/cooperativity between ensembles of cross-bridge states (27,34–36) is therefore minimized under these conditions, which limit the concentration of various actomyosin cross-bridge states. Populated weakly or nonstereospecifically bound states without a significant stiffness signal are mechanically invisible—particularly so in the absence of movement, a signature feature of T-jump experiments. These properties, and the fact that thin filaments are saturated with myosin renders two-state tension generation immune to influences like temperature-induced changes in the distribution of adjacent intermediate states. If they did, the system would not appear two-state.

Relationship between τ_3 and de novo tension generation by τ_2

Rate data is required to exclude τ_3 (equivalent of the L-jump phase 4, the slow asymptotic return to the prejump tension) from tension generation to leave τ_2 as the sole de novo tension generating step (1,10,16). We know from the τ_2 and τ_3 amplitude data that the entire tension rise is generated either by 1), a single, shared two-state transition; or 2), two separate but identical two-state transitions. If the first assumption is true, the kinetics of the fastest phase τ_2 alone will be two-state; if the second assumption is true, both τ_2 and τ_3 will show two-state behavior.

We first modeled this phase as a rapid, temperature-sensitive equilibrium early in the cycle separated from tension generation (τ_2) by a slow temperature-independent step with the properties of τ_3 (16). However, the remarkable discovery of a fixed 1:0.75 ratio between the amplitudes of τ_3 and τ_2 alluded to above, pointed to a stoichiometric, cooperative link between τ_2 and τ_3 (1). We have hypothesized that τ_3 reflects the diffusion-limited attachment of the second head of myosin after tension generation by the first (1). Strain-dependent changes in subunit repeat of the thick and thin filaments might also contribute to the phenomenon (37,38). Whatever the exact mechanism, a pool of MDP heads is a prerequisite for the functioning of τ_3. Direct evidence for a large reserve population of detached MDP heads prevented from interacting with thin filaments fully saturated with myosin comes from P_i burst experiments (39,40). At 20°C in relaxed fibers, the P_i burst is 1.0 with the MDP state equal to the concentration of myosin heads. During isometric contraction, the P_i burst drops to ~0.5, and with unconstrained acto-S1, it is zero. Thus, under our conditions, roughly half the myosin heads are detached in the MDP state with the other half bound to actin. The zero burst with acto-S1 highlights the affinity of the MDP intermediate for actin, and the inhibitory constraints on the reaction introduced by sarcomere structure. Without mechanical constraint by the structure of the sarcomere, there would be no τ_3—it is important to note that the phase appears absent in single molecule experiments (41). As mentioned, the location of the tension-generating step in the cross-bridge cycle is controversial. Opinion is divided as to whether the transition occurs before (4–6), during (7,8), or after (9–13) P_i release. As detailed in a series of articles (1,10–12,16), we favor a mechanism in which tension generation occurs isolated from the biochemistry as an isomerization between strongly-bound AMD cross-bridge states.

Mechanism of tension generation

Experiment suggests that tension generation in muscle is an endothermic order-disorder transition associated with the slow component of the Huxley-Simmons phase 2 in L-jump experiments and its equivalent, phase τ_2, in T-jump experiments. This observation is in accord with calorimetric measurements of heat absorption during phase 2 tension recovery after a step-release in L-jump experiments (42). Here, we consider specific physical properties of this reaction to gain deeper insight into mechanism.

Rates of simple chemical reactions normally accelerate with increasing temperature. In our experiments, tension generation follows normal Arrhenius behavior with k_1 accelerated by increasing temperature, while the reverse reaction shows anti-Arrhenius behavior (negative $\Delta H^{\ddagger}$) with k_{-1} slowed by increasing temperature. For simple reactions, transition-state entropy values can be either negative or positive, but transition-state enthalpy values are always positive. This follows from the fact that bond-breaking energy is required to reach the transition (saddle) state. Among all protein-associated biological reactions, protein folding alone exhibits the anti-Arrhenius kinetics we observe for the reversal of tension generation, e.g., (43–46). Anomalous kinetics like this are considered an intrinsic property of the high complexity of protein folding process, not the breaking of physical laws. At the macroscopic level, classical studies correctly ascribed such behavior to differential changes in the temperature-dependent heat capacities (ΔC_p) of the unfolded, transition and folded states (22). This treatment

contrasts with the emerging ''new view'' of the mechanism of protein folding based on energy surfaces or landscapes that define protein folding as the progressive organization of a large ensemble of unfolded states folding along a multiplicity of pathways (see (47) and references therein). At its simplest, this energy landscape is often visualized as a funnel with a wide mouth to symbolize the multitude of states occupied by the unfolded state. The transition state is then visualized as a reduced number of states situated part-way down the funnel (i.e., not the classical rare high energy intermediate, but a ''constriction'' in the number of states), with the native state occupying fewer microstates at the funnel base. This microscopic formulation of the folding/unfolding of a small protein provides deeper insight into mechanism, and has recently led to a quantitative kinetic formulation of the pathway. High resolution data of the two-state folding of small proteins typically shows Arrhenius plots with upward curvature for unfolding, and anti-Arrhenius plots with downward curvature for folding e.g., (22,43,45). These distinctive non-Arrhenius features have recently been successfully simulated with multiple parallel pathways where temperature differentially affects the number of microscopic states populated by the unfolded, transition, and folded states of the protein (48). Increasing temperature causes the greatest increase in the number of unfolded microstates, followed by the transition, and folded states in decreasing order. This model is useful because it provides a conceptual framework for the conformational changes that could mediate tension generation. Our Arrhenius plots exhibit Arrhenius/anti-Arrhenius behavior, but not the curvatures—simulation shows that a large $\Delta C_p > \sim 2$ kJ mol^{-1} K^{-1} would be required to detect this curvature under our experimental conditions. Empirically, the Arrhenius/anti-Arrhenius plots we record (Fig. 5) with positive unfolding $\Delta H^{\ddagger}$ values and a negative folding $\Delta H^{\ddagger}$ values most closely resemble recent laser T-jump studies on the unfolding/folding of protein tertiary structure (triple-helix (46)) and secondary structure (α-helix (44,46) and a β-hairpin (49)). These various observations open up the possibility that a subclass of endothermic order-disorder reactions, characterized by multistate/multipathway kinetics, could function to create the tension-generating state. It is intriguing to consider how these insights might relate to the bending of the β-sheet core of the myosin head, SH1-helix melting, and other associated changes recently invoked in structural models of tension generation (50,51).

In the swinging lever-arm mechanism of tension generation (2), the proximal catalytic domain of the myosin head is firmly attached to actin, while the distal lever-arm domain swings to generate tension and movement. Our findings support this model by excluding movement of the catalytic domain on actin during tension generation for the following reason: Cross-bridge stiffness remains constant as the occupancy of the pre-tension-generating and tension-generating states changes with temperature. Contrary to a recent assertion of ours (12), we find fiber stiffness to be independent of temperature at and above 5°C when the correct tension-temperature data of Fig. 1 is used to calculate absolute stiffness values (unpublished). This confirms literature reports of decreased stiffness at low temperatures and a constant stiffness at higher temperatures in rat muscle fibers (33). Collectively, these observations exclude (barring a compensatory structural change) large changes in bond strength between the catalytic domain of myosin and actin when the pre-force-generating state converts to the tension-generating state on increasing fiber temperature. No change in stiffness also excludes a subclass of folding/unfolding reactions from tension generation. Thus, the direct functioning of helix-coil-like transitions in which rigid helix unfolds to a tension-generating, compliant, random-coil are excluded from function (26). Thus, a conformational change involving local unfolding of cross-bridge tertiary/secondary structure coupled to the rigid body movements described in structural studies (2) provides a plausible mechanism of contraction. To the best of our knowledge, this is the first example of the adaptation of a conformational change involving Arrhenius/anti-Arrhenius kinetics to function.

CONCLUSIONS

Under special experimental conditions, a causal relationship exists between fiber tension and the kinetics of the T-jump phase τ_2. By extension, this finding applies to phase 2_{slow}, a subcomponent of the classical L-jump Huxley-Simmons phase 2, which has been fundamental to the study of tension generation in muscle for over 35 years. Single-step two-state tension generation fits a mechanism in which the power-stroke is a mechanical property of the tension-generating state, an observation entirely consistent with single molecule experiments on striated muscle myosin in which tension is produced in an abrupt single step (41). Two-step tension generation with smooth muscle myosins and other myosins (52), consisting of a major step and a control substep, would be a functional elaboration on this basic theme. Thus, single-step tension generation appears to be the canonical mechanism for tension generation. As mentioned earlier, various kinetic observations strongly indicate that this transition occurs between AMD states (1,10–12,16). Arrhenius behavior for tension generation and anti-Arrhenius behavior for its reversal show a process related to protein unfolding. It therefore appears likely that a multistate/multipathway conformational change that resembles protein unfolding/folding, mediates tension generation in the actomyosin cross-bridge. At physiological temperatures, force production is thus potentiated by the acceleration of the forward rate constant of tension generation, and a counter-slowing of the reverse rate constant of tension generation, by increasing temperature. It also implies that raising fiber temperature will serve to concentrate cross-bridges in the tension-generating state, aiding structural studies of this otherwise elusive intermediate.

We thank Drs. Tom Barman, William A. Eaton, Bertrand García-Moreno E., Kenneth C. Holmes, Steve Winitsky, and Leepo Yu for discussions and comments.

REFERENCES

1. Davis, J. S. 1998. Force generation simplified. Insights from laser temperature-jump experiments on contracting muscle fibers. *Adv. Exp. Med. Biol.* 453:343–351 (discussion 351–342).
2. Geeves, M. A., and K. C. Holmes. 1999. Structural mechanism of muscle contraction. *Annu. Rev. Biochem.* 68:687–728.
3. White, H. D., and E. W. Taylor. 1976. Energetics and mechanism of actomyosin adenosine triphosphatase. *Biochemistry.* 15:5818–5826.
4. Kawai, M., and H. R. Halvorson. 1991. Two step mechanism of phosphate release and the mechanism of force generation in chemically skinned fibers of rabbit psoas muscle. *Biophys. J.* 59:329–342.
5. Dantzig, J. A., Y. E. Goldman, N. C. Millar, J. Lacktis, and E. Homsher. 1992. Reversal of the cross-bridge force-generating transition by photogeneration of phosphate in rabbit psoas muscle fibers. *J. Physiol.* (*Lond.*). 451:247–278.
6. Tesi, C., F. Colomo, N. Piroddi, and C. Poggesi. 2002. Characterization of the cross-bridge force-generating step using inorganic phosphate and BDM in myofibrils from rabbit skeletal muscles. *J. Physiol.* 541:187–199.
7. Eisenberg, E., and T. L. Hill. 1985. Muscle contraction and free energy transduction in biological systems. *Science.* 227:999–1006.
8. Baker, J. E. 2004. Free energy transduction in a chemical motor model. *J. Theor. Biol.* 228:467–476.
9. Howard, J. 2001. Mechanics of Motor Proteins and the Cytoskeleton. Sinauer Associates, Sunderland, MA.
10. Davis, J. S., and W. F. Harrington. 1993. A single order-disorder transition generates tension during the Huxley-Simmons phase 2 in muscle. *Biophys. J.* 65:1886–1898.
11. Davis, J. S., and M. E. Rodgers. 1995. Indirect coupling of phosphate release and de novo tension generation during muscle contraction. *Proc. Natl. Acad. Sci. USA.* 92:10482–10486.
12. Davis, J. S., and N. D. Epstein. 2003. Kinetic effects of fiber type on the two subcomponents of the Huxley-Simmons phase 2 in muscle. *Biophys. J.* 85:390–401.
13. Spudich, J. A. 2001. The myosin swinging cross-bridge model. *Nat. Rev. Mol. Cell Biol.* 2:387–392.
14. Homsher, E., and N. C. Millar. 1990. Caged compounds and striated muscle contraction. *Annu. Rev. Physiol.* 52:875–896.
15. Davis, J. S. 2000. Kinetic analysis of dynamics of muscle function. *Methods Enzymol.* 321:23–37.
16. Davis, J. S., and M. E. Rodgers. 1995. Force generation and temperature-jump and length-jump tension transients in muscle fibers. *Biophys. J.* 68:2032–2040.
17. Davis, J. S., and N. D. Epstein. 2005. Identification and quantitative characterization of the kinetic source of tension in muscle. 2005 Biophysical Society Meeting Abstracts. *Biophys. J. Suppl:Abstr.* 619-Pos.
18. Kawai, M., K. Kawaguchi, M. Saito, and S. Ishiwata. 2000. Temperature change does not affect force between single actin filaments and HMM from rabbit muscles. *Biophys. J.* 78:3112–3119.
19. Kawaguchi, K., and S. Ishiwata. 2001. Thermal activation of single kinesin molecules with temperature pulse microscopy. *Cell Motil. Cytoskeleton.* 49:41–47.
20. Bernasconi, C. F. 1976. Relaxation Kinetics. Academic Press, New York.
21. Gutfreund, H. 1995. Kinetics for the Life Sciences: Receptors, Transmitters and Catalysts. Cambridge University Press, Cambridge.
22. Fersht, A. R. 1999. Structure and Mechanism in Protein Science: A Guide to Enzyme Catalysis and Protein Folding. W. H. Freeman and Company, New York.
23. Ranatunga, K. W. 1996. Endothermic force generation in fast and slow mammalian (rabbit) muscle fibers. *Biophys. J.* 71:1905–1913.
24. Coupland, M. E., E. Puchert, and K. W. Ranatunga. 2001. Temperature dependence of active tension in mammalian (rabbit psoas) muscle fibers: effect of inorganic phosphate. *J. Physiol.* 536:879–891.
25. Goldman, Y. E., J. A. McCray, and K. W. Ranatunga. 1987. Transient tension changes initiated by laser temperature jumps in rabbit psoas muscle fibers. *J. Physiol.* (*Lond.*). 392:71–95.
26. Davis, J. S., and W. F. Harrington. 1987. Force generation by muscle fibers in rigor: a laser temperature-jump study. *Proc. Natl. Acad. Sci. USA.* 84:975–979.
27. Huxley, A. F., and R. M. Simmons. 1971. Proposed mechanism of force generation in striated muscle. *Nature.* 233:533–538.
28. Pate, E., K. Franks-Skiba, H. White, and R. Cooke. 1993. The use of differing nucleotides to investigate cross-bridge kinetics. *J. Biol. Chem.* 268:10046–10053.
29. Webb, M. R., M. G. Hibberd, Y. E. Goldman, and D. R. Trentham. 1986. Oxygen exchange between Pi in the medium and water during ATP hydrolysis mediated by skinned fibers from rabbit skeletal muscle. Evidence for Pi binding to a force-generating state. *J. Biol. Chem.* 261:15557–15564.
30. Cooke, R., M. S. Crowder, and D. D. Thomas. 1982. Orientation of spin labels attached to cross-bridges in contracting muscle fibers. *Nature.* 300:776–778.
31. Nyitrai, M., and M. A. Geeves. 2004. Adenosine diphosphate and strain sensitivity in myosin motors. *Philos. Trans. R. Soc. Lond. B Biol. Sci.* 359:1867–1877.
32. Taylor, E. W. 1977. Transient phase of adenosine triphosphate hydrolysis by myosin, heavy meromyosin, and subfragment 1. *Biochemistry.* 16: 732–739.
33. Galler, S., and K. Hilber. 1998. Tension/stiffness ratio of skinned rat skeletal muscle fiber types at various temperatures. *Acta Physiol. Scand.* 162:119–126.
34. Vilfan, A., and T. Duke. 2003. Instabilities in the transient response of muscle. *Biophys. J.* 85:818–827.
35. Duke, T. A. 1999. Molecular model of muscle contraction. *Proc. Natl. Acad. Sci. USA.* 96:2770–2775.
36. Lan, G., and S. X. Sun. 2005. Dynamics of myosin-driven skeletal muscle contraction: I. Steady-state force generation. *Biophys. J.* 88: 4107–4117.
37. Chase, P. B., J. M. Macpherson, and T. L. Daniel. 2004. A spatially explicit nanomechanical model of the half-sarcomere: myofilament compliance affects Ca^{2+}-activation. *Ann. Biomed. Eng.* 32:1559–1568.
38. Martyn, D. A., P. B. Chase, M. Regnier, and A. M. Gordon. 2002. A simple model with myofilament compliance predicts activation-dependent cross-bridge kinetics in skinned skeletal fibers. *Biophys. J.* 83:3425–3434.
39. Lionne, C., M. Brune, M. R. Webb, F. Travers, and T. Barman. 1995. Time-resolved measurements show that phosphate release is the rate-limiting step on myofibrillar ATPases. *FEBS Lett.* 364:59–62.
40. Lionne, C., B. Iorga, R. Candau, N. Piroddi, M. R. Webb, A. Belus, F. Travers, and T. Barman. 2002. Evidence that phosphate release is the rate-limiting step on the overall ATPase of psoas myofibrils prevented from shortening by chemical cross-linking. *Biochemistry.* 41: 13297–13308.
41. Finer, J. T., R. M. Simmons, and J. A. Spudich. 1994. Single myosin molecule mechanics: picoNewton forces and nanometer steps. *Nature.* 368:113–119.
42. Gilbert, S. H., and L. E. Ford. 1988. Heat changes during transient tension responses to small releases in active frog muscle. *Biophys. J.* 54:611–617.
43. Oliveberg, M., Y. J. Tan, and A. R. Fersht. 1995. Negative activation enthalpies in the kinetics of protein folding. *Proc. Natl. Acad. Sci. USA.* 92:8926–8929.
44. Lednev, I. K., A. S. Karnoup, M. C. Sparrow, and S. A. Asher. 1999. Alpha-helix peptide folding and unfolding activation barriers: A nanosecond UV resonance Raman study. *J. Am. Chem. Soc.* 121:8074–8086.

45. Zhu, Y., D. O. Alonso, K. Maki, C. Y. Huang, S. J. Lahr, V. Daggett, H. Roder, W. F. DeGrado, and F. Gai. 2003. Ultrafast folding of α3D: a de novo designed three-helix bundle protein. *Proc. Natl. Acad. Sci. USA.* 100:15486–15491.

46. Vu, D. M., J. K. Myers, T. G. Oas, and R. B. Dyer. 2004. Probing the folding and unfolding dynamics of secondary and tertiary structures in a three-helix bundle protein. *Biochemistry.* 43:3582–3589.

47. Onuchic, J. N., and P. G. Wolynes. 2004. Theory of protein folding. *Curr. Opin. Struct. Biol.* 14:70–75.

48. Zaman, M. H., T. R. Sosnick, and S. R. Berry. 2003. Temperature dependence of reactions with multiple pathways. *Phys. Chem. Chem. Phys.* 5:2589–2594.

49. Munoz, V., P. A. Thompson, J. Hofrichter, and W. A. Eaton. 1997. Folding dynamics and mechanism of β-hairpin formation. *Nature.* 390:196–199.

50. Holmes, K. C., I. Angert, F. J. Kull, W. Jahn, and R. R. Schroder. 2003. Electron cryo-microscopy shows how strong binding of myosin to actin releases nucleotide. *Nature.* 425:423–427.

51. Coureux, P. D., A. L. Wells, J. Menetrey, C. M. Yengo, C. A. Morris, H. L. Sweeney, and A. Houdusse. 2003. A structural state of the myosin V motor without bound nucleotide. *Nature.* 425:419–423.

52. Veigel, C., L. M. Coluccio, J. D. Jontes, J. C. Sparrow, R. A. Milligan, and J. E. Molloy. 1999. The motor protein myosin-I produces its working stroke in two steps. *Nature.* 398:530–533.